Available online at www.sciencedirect.com
SCIENCE DIRECT®
International Journal of Heat and Mass Transfer 48 (2005) 4590–4597
International Journal of HEAT and MASS TRANSFER
www.elsevier.com/locate/ijhmt

Critical heat flux of steady boiling for saturated liquids jet impinging on the stagnation zone

Yu-hao Qiu, Zhen-hua Liu *

School of Mechanical and Power Engineering, Shanghai Jiaotong University, Shanghai 200030, PR China

Received 4 April 2004; received in revised form 3 February 2005

Abstract

An experimental investigation was carried out for predicting the critical heat flux (CHF) of convective boiling of saturated liquids for a round jet impinging on the horizontal jet stagnation zone. The model of maximum liquid subfilm thickness based on the Helmholtz instability was used to derive a semi-theoretical equation. The experimental data of four liquids: water, ethanol, R-113 and R-11 were employed to determine the correlation factor. The impact velocity ranged from 0.5 m/s to 10 m/s and the diameters of the jet nozzle ranged from 3 mm to 10 mm. A semi-theoretical correlation was proposed for predicting CHF of convective boiling for saturated liquids jet impinging on the stagnation zone in a wide range.

Keywords: Boiling; Evaporation; Jets; Heat transfer; CHF

1. Introduction

Liquid jet impinging cooling of hot plate, as a highly effective cooling method, has been widely used in iron and steel industry, nuclear power process and many microelectronic devices making and thermal management processes. According to the ranges of plate temperatures, the heat transfer modes may be divided into forced convection, nucleate boiling, transition boiling and film boiling. For liquid jet impinging boiling on the hot plate, the assessment of the critical heat flux (CHF) is very important to understand the burnout phenomenon in nucleate boiling and represents the largest cooling capacity for the jet cooling. The geometries of a liquid jet impinging on a horizontal hot plate can be divided into two modes. One mode is the free film flow as shown in Fig. 1(a) named as the mode A in this paper, in which a great heated disk or rectangular plate is cooled by a small liquid jet and the ratio of the heated disk diameter to the nozzle diameter is much larger than unity. In general, for this geometry condition, the jet impinging cooling experiments can be only carried out for the forced convection and nucleate boiling heat transfer regimes. After the boiling critical crisis occurred, the heat-transfer surface would be divided into two zones of the jet stagnation zone and dry-out zone and hence the temperature and heat flux of the heat-transfer surface would be not uniform. The second mode is the stagnation jet flow as shown in Fig. 1(b) named as the mode B in this paper, in which the heat-transfer surface and the jet nozzle have a same diameter and the

* Corresponding author. Tel.: +86 21 62932992; fax: +86 21 62933086.
E-mail address: liuzhenh@sjtu.edu.cn (Z.-h. Liu).

0017-9310/$ - see front matter © 2005 Published by Elsevier Ltd.
doi:10.1016/j.ijheatmasstransfer.2005.06.002

Nomenclature

c	correlation factor (–)
d	diameter of jet nozzle or the heated surface in mode B (m)
d_n	diameter of jet nozzle in mode A (m)
D	diameter of the heated surface in mode A (m)
g	gravitational acceleration (m s^{-2})
G	mass flux of liquid jet, $\rho_l V$ (kg m^{-2} s^{-1})
h	heat transfer coefficient (W m^{-2} K^{-1})
h_{fg}	latent heat of evaporation (J kg^{-1})
q	wall heat flux (J m^{-2} s^{-1})
$q_{c,0}$	critical heat flux for saturated liquid (J m^{-2} s^{-1})
P	pressure (Pa)
Pr	Prandtl number (–)
v	impact velocity of jet flow at nozzle exit (m s^{-1})

Greek symbols

ΔT	wall superheat (K)
λ	thermal conductibility (W m^{-1} s^{-1})
ν	cinematic viscosity (m^2 s^{-1})
ρ	density (kg m^{-3})
σ	surface tension (N m^{-1})

Subscripts

l	liquid
v	vapor

heat-transfer surface is in the jet stagnation zone. For this geometry condition, the jet impinging cooling experiments can be extensively carried out in total boiling regimes including transition and film boiling with uniform wall temperatures and wall heat fluxes.

In the past two decades, for the mode A, The studies associated with CHF of saturated and sub-cooled liquids on the disk or rectangular plate have been performed extensively. A variety of the experimental results have been reported and various semi-theoretical correlations and empirical correlations have been proposed for predicting CHF for different parameter ranges such as impact velocities, ratios of liquid density to vapor density, heater geometries and multiple jet systems [1–11].

For the jet impinging boiling of the mode A, the mechanism of the burnout is evidenced to be the dry-out of the free flow liquid film, which is assumed to be equal or proportional to the maximum liquid subfilm thickness proposed by Haramura and Katto [12], at the edge of the heat-transfer surface. The dry-out phenomenon takes place firstly at the edge of the heat-transfer surface and extends rapidly to whole free flow zone. After burnout phenomenon occurred, only the stagnation zone could be impinged directly by current flow and liquid flow would be splashed completely off the heat-transfer surface at the edge of the stagnation zone along the radial direction. Following equation could be derived theoretically using the model of maximum liquid subfilm thickness for the mode A [5].

$$\frac{q_{c,0}}{Gh_{fg}} = 0.280\left(\frac{\rho_v}{\rho_l}\right)^{0.467}\left(1+\frac{\rho_v}{\rho_l}\right)^{1/3} \times \left(\frac{\sigma\rho_l}{G^2(D-d_n)}\right)^{1/3}\left(1+\frac{D}{d_n}\right)^{-1/3} \quad (1)$$

Monde et al. [10] proposed a simply empirical correlation as follow:

$$\frac{q_{c,0}}{Gh_{fg}} = 0.278\left(\frac{\rho_v}{\rho_l}\right)^{0.645}\left(\frac{\sigma\rho_l}{G^2(D-d_n)}\right)^{0.343}\left(1+\frac{D}{d_n}\right)^{-0.343} \quad (2)$$

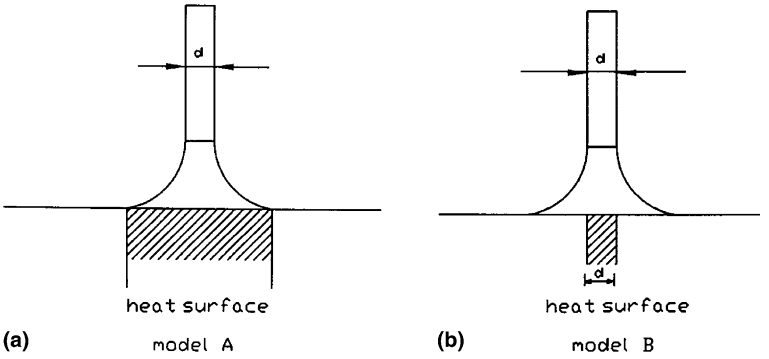

Fig. 1. The schematic diagram of the physical model: (a) the mode A and (b) the mode B.

where D and d_n denote the heated disk diameter and the nozzle diameter, respectively. G denotes the mass flux of jet flow. The applicable range of D/d_n has not been defined clearly for the above two correlations. It is evident that the above correlations can not been used to the mode B, in which D/d_n is equal to or less than unity and jet boiling is limited in the stagnation zone.

Comparing with the mode A, the studies of the critical heat flux for the mode B are insufficient. These studies focused mainly on the boiling heat transfer of sub-cooled water [13–18]. A few data of CHF were included in the experimental results for the nucleate boiling heat transfer. Recently, Liu and co-workers carried out theoretical and experimental studies concerning the CHF of the mode B using the saturated water and sub-cooled water [19,20]. In their studies, a theoretical CHF model, which is similar to that of the maximum liquid subfilm thickness proposed by Haramura and Katto [12], was employed and a semi-theoretical correlation was proposed for predicting the CHF of the saturated liquids as the follows:

$$\frac{q_{c,0}}{Gh_{fg}} = c\left(1+\frac{\rho_v}{\rho_l}\right)^{\frac{1}{3}}\left(\frac{\sigma\rho_l}{G^2 d}\right)^{\frac{1}{3}}\left(\frac{\rho_v}{\rho_l}\right)^{\frac{1.4}{3}} \tag{3}$$

where G is equal to $\rho_l V$. C is a correlation factor and it could be determined from the experimental data. Because the physical properties are constants for the various saturated liquids at a fixed test pressure, by rewriting Eq. (3), we get

$$q_{c,0} \propto \left(\frac{V}{d}\right)^{1/3} \tag{4}$$

In the study of Liu and Zhu [19] for the saturated water jet on a stainless steel foil heated directly by a DC power supply, the following correlation was obtained at atmospheric pressure condition.

$$q_{c,0} = 0.36\times 10^6\left(\frac{V}{d}\right)^{1/3} \tag{5}$$

From Eq. (4), the correlation factor in Eq. (3) can be determined as 0.132 for the saturated water.

Up to now, the fundamental data of CHF of the mode B is poor still. No any data from liquids expect water can be employed to check Eq. (3). It is still unknown that whether Eq. (3) is available in a wide range when the working substances or the physical properties change.

In the present study, an experimental study was carried out for investigating the CHF of convective boiling of various saturated liquids including water for a round jet impinging on the steady heated stagnation zone which has the same diameter as that of the jet nozzle (model B). The form of Eq. (3) is still employed as a fundamental correlation for predicting the CHF of the model B for various liquids. The effects of the physical properties on the correlation factor and the exponents of the correlation were investigated in wide range. Finally, a correlation was proposed for predicting CHF of the model B for various saturated liquids.

2. Experimental apparatus

In this study, steady heat transfer experiments were carried out for the nucleate boiling regime to obtain boiling curves and determine critical heat fluxes in the steady state. Fig. 2 shows the schematic diagram of the experimental apparatus. It mainly consisted of the heating block, the circulation system of water, the measuring devices and electric power supply. Fig. 3 shows the schematic diagram of the test box, in which a heated block was mounted. The heated block was a vertical copper bar having 50 mm diameter and 120 mm height, whose top surface was a smooth, horizontally circular heat-transfer surface, and it was heated with a ribbon electric heater (main heater) twisted outside of the copper bar. The isinglass sheet was used as the insulator between the copper bar and main heater. The copper bar was placed in a thick ceramic tube; a ribbon electric heater (auxiliary heater) was twisted outside of the ceramic tube for preventing the heat losses from the heated block. Six different sizes of circular heat-transfer surfaces with diameters from 12 mm to 3 mm were used in this experiment and they corresponded to four round nozzles with the same diameters. In the upper column of the copper bar, three Φ0.1 mm thermocouples were horizontally inserted at the center axial line of the copper bar. The distances between the thermocouples were 3.0 mm and the distance between the top thermocouples and the heat-transfer surface was 2.0 mm. Signals from the thermocouples mounted in the copper bar were measured by a digital voltmeter and then fed into a computer, which converted them to wall temperature and wall flux using a steady one-dimensional thermal conduction equation along the vertical direction. One of them was fed into a PID temperature controller as a feed back signal, which then adjusted the power supply. In the tests, the electric power of the auxiliary heater was carefully adjusted for preventing the heat losses from the main heater. The test box made of stainless steel and had a diameter of 250 mm and a height of 200 mm. The space inside the test box was filled by asbestos. All of the measurements were performed in the steady state, the temperature and heat flux of the heat-transfer surface were calculated from the temperature difference between two thermocouples mounted on the center axial line of the copper bar. An alarm thermocouples inserted at the bottom of the copper bar was connected to a temperature controller that prevents the maximum temperature of the copper bar from exceeding 700 °C. In this experiment, it has been confirmed that

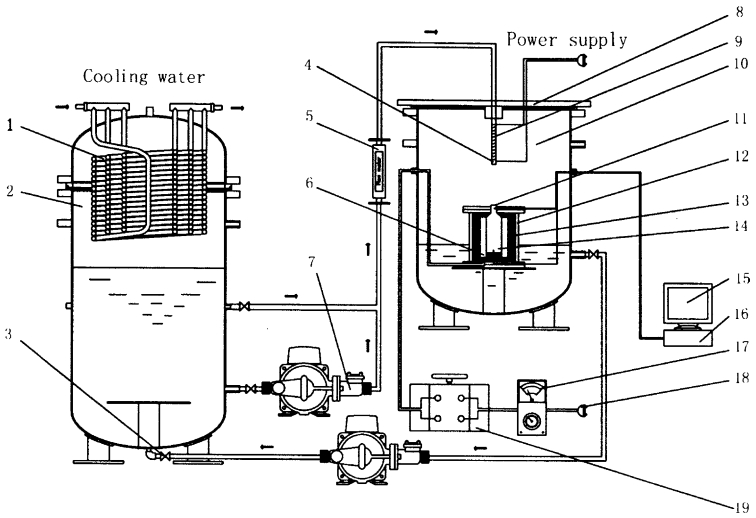

1 Condenser
2 Water tank
3 Valve
4 Nozzle
5 Flow meter
6 Heater
7 Pump
8 Support board
9 Heating resistance coil
10 Test vessel
11 Heat transfer surface
12 Test box
13 Asbestos wool
14 Copper column
15 Computer
16 Digital acquisition system
17 Temperature controller
18 Power supply
19 Transformer

Fig. 2. The schematic diagram of the experimental apparatus.

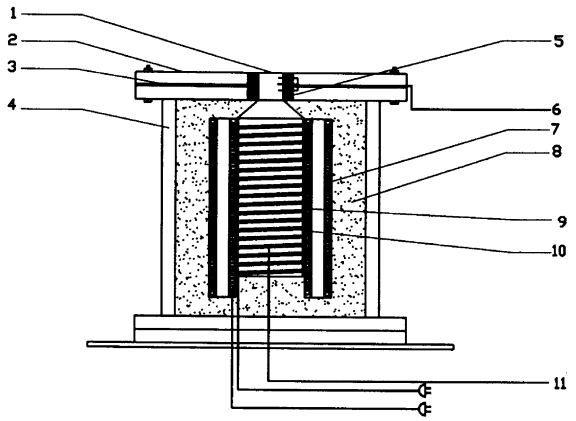

1 Heat transfer surface
2 Cover board
3 Latex sheet
4 Text box
5 Sealed silica gel
6 Measuring thermocouples
7 Asbestos
8 Auxiliary heater
9 Isinglass
10 Main heater
11 Alarm thermocouples

Fig. 3. The schematic diagram of a heated specimen.

the assumption of one-dimensional heat conduction is essentially satisfied in the upper column of the copper bar by a numerical simulation and test results.

Ion-exchanged water (the maximum electric conductivity was less than 10 $(\mu\Omega\,\mathrm{cm})^{-1}$ in the experiments), chemical-pure ethanol, R-113 and R-11 were used as the test liquids. The test liquid was heated to be close to the saturation temperature under atmospheric pressure in the high-level water tank, which was fitted with two immersion heaters on its bottom section and a reflux condenser mounted above the tank. Then, the test liquid was drained from the liquid tank by a pump, passed through a regulating valve and a flow meter into the jet nozzle made of a long copper glass tube, in which the test liquid was heated to the saturation temperature by a heater amounted on the nozzle and the temperature of the test liquid was measured by the thermocouple, the liquid jet impinged onto the heat-transfer surface, then was drained into a drain tank to be recycled. The distance between the heat-transfer surface and the nozzle was fixed at 5.0 mm in all tests. Prior to the formal tests, it has been affirmed that the distance between the heat-transfer surface and the nozzle has no effect on the jet boiling characteristics.

During operation, electric power was increased gradually. The computer not only measured the wall temperature and wall heat flux instantaneously, but also gave an alarm when the wall temperature increased quickly

Table 1
Experimental conditions in the present study

Test fluid	Water, ethanol, R-113, R-11
Heating condition	Steady state, constant wall heat flux
Test pressure	Atmospheric pressure
Impact velocity (m/s)	0.5–10
Nozzle diameter (mm)	3, 4, 6, 8, 10, 12
Jet height (m)	0.05
Substrate	Copper block for all

and did not attain a steady state. Such an alarm means that the boiling crisis has occurred; therefore, the electric power was cut automatically off. After the boiling crisis occurred, the test was repeated from the steady state of the former time, the output electric power increased slowly in an increment of 2% of the electric power of the former time. When the boiling crisis occurred again, the test was stopped and the wall heat flux of the former time was determined as the critical heat flux.

Table 1 shows the experimental conditions. In this experiment, the impact velocity of water ranged 0.5 m/s to 10 m/s, and, the wave of the impact velocity was limited within ±4%. Six different specimens with cross-section diameters from 12 mm to 3 mm were used in this experiment and they corresponded to four the same round jet nozzle diameters, respectively. The impact velocity was calculated with an accuracy of 2% of reading, associated with the measurement of the liquid flow rate. The calibration errors of the thermocouples were less than 0.2 K. The liquid jet temperature was measured with an accuracy of 0.2 K. The maximum location deviation between thermocouples was about 0.1 mm. The maximum uncertainties of the wall superheat and wall heat flux were about 12%. The maximum uncertainty of the critical heat flux was 13%. In special, for the tests used water, the maximum uncertainty of the critical heat flux was 4%.

3. Results and discussion

Fig. 4 shows some samples of the temperature distributions in the upper column of the copper bar at different experimental conditions. The temperatures measured by the thermocouples are on the abscissa, and the distances from the wall along the vertical direction are on the ordinate. The measured results clearly show linear temperature distributions along the vertical direction in the upper column of the copper bar.

Fig. 5 shows a sample of the experimental results of fully developed nucleate boiling regime at the stagnation zone for ethanol jet using the jet diameter of 8 mm. Heat transfer data are plotted in the form of boiling curves (wall heat flux against wall superheat) for different impact velocities.

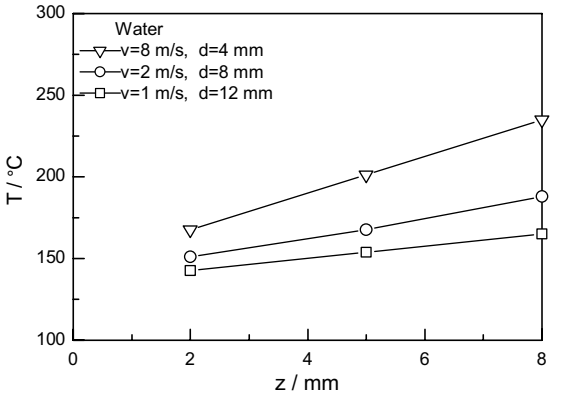

Fig. 4. Temperature distributions of thermocouples in the heated body.

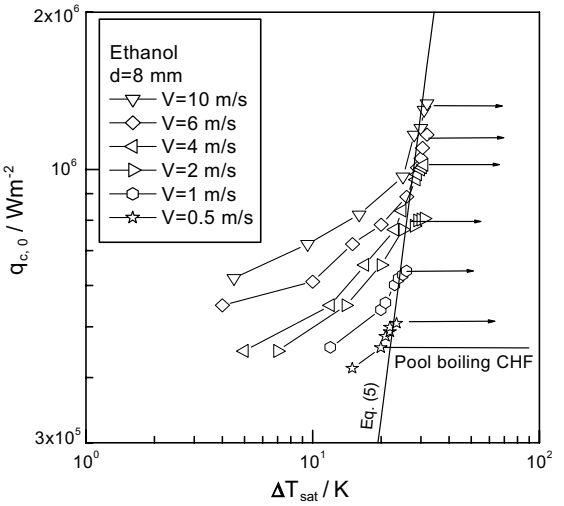

Fig. 5. Boiling curves of saturated ethanol jet for $\Phi 8$ mm nozzle.

Kutateladze's empirical correlation [21] is also shown in Fig. 5 in form of solid lines for comparison

$$\frac{h}{\lambda_l}\sqrt{\frac{\sigma}{g(\rho_l-\rho_v)}} = 7.0\times10^{-4}Pr_l^{0.35}\left[\frac{q}{\rho_v h_{fg} v_l}\sqrt{\frac{\sigma}{g(\rho_l-\rho_v)}}\right]^{0.7}\left[\frac{p}{\sigma}\sqrt{\frac{\sigma}{g(\rho_l-\rho_v)}}\right]^{0.7} \quad (6)$$

It is clear from Eq. (6) that prior to fully developed nucleate boiling, higher velocities increase the heat transfer coefficient and delay boiling incipience. Because the objective of this study is investigation of the CHF, hence, the other experimental data for various test liquids have not been presented in this paper.

In fully developed nucleate boiling regime, the data resulted from different impact velocities generally converged into essentially the pool nucleate boiling curve. The data for different liquids are reasonably well agreement with the Eq. (6) and are rather higher than the calculated values. These deviations may be resulted from the different surface configurations such as surface roughness. The insensitivity of the boiling curve to changes in compact velocity indicates that heat transfer in the fully developed nucleate boiling regime is dominated by bubble activity at the surface, regardless of the contribution of single-phase turbulent transport in the bulk flow. This phenomenon is similar to other forced convective boiling characteristics. However, the effect of impact velocity is become more significant at the CHF, which is delayed with increasing impact velocity. This trend is attributed to increased liquid-solid contact with the hot surface and decreased void fraction in the liquid flow. Not shown here, the CHF is also delayed with decreasing jet diameter. This trend is attributed to decreased flow distance of the incoming liquid though the liquid subfilm layer.

By Eq. (4), in theoretical, there exists a linear relation between the CHF and $(v/d)^{1/3}$. Fig. 6(a)–(d) show the experimental results of the effects of (v/d) on the CHF for four test liquids. One CHF data of R-113 proposed by Ma and Bergles [15] are also shown for comparison in Fig. 6(c). It is found that there exists a good linear relation between the CHF data and $(v/d)^{1/3}$ for all liquids. Therefore, the form of Eq. (4) resulted from the theoretical resolution is available.

For the case the test pressure is greatly lower than the critical pressure, the term of $(1+\rho_v/\rho_l)^{1/3}$ in Eq. (3) is very close to unity, therefore, $q_{c,0}$ would be the function of (ρ_v/ρ_l). Fig. 7 shows the effect of (ρ_v/ρ_l) on the CHF using the present experimental data. It is also found that there exists a good linear relation between the dimensionless CHF data and $(\rho_v/\rho_l)^{1.4/3}$. Therefore, the form of Eq. (3) is available in a wide range tested. It is confirmed from the experimental data that the exponents in Eq. (3) are correct; the further work is to determine the correlation factor in Eq. (3).

By using a least-square fit, the correlation factor in Eq. (3) was determined from the experimental data of CHF obtained in the present study (82 data). Good agreement between the CHF data and the prediction is obtained for $C=0.130$. Table 2 shows the errors of the CHF predications by Eq. (7).

$$\frac{q_{c,0}}{Gh_{fg}} = 0.130\left(1+\frac{\rho_v}{\rho_l}\right)^{1/3}\left(\frac{\sigma\rho_l}{G^2 d}\right)^{1/3}\left(\frac{\rho_v}{\rho_l}\right)^{1.4/3} \tag{7}$$

The correlation factor in Eq. (7) is less 2% than that in Eq. (5). Eq. (7) resulted from a copper surface test is very close to Eq. (5) resulted from a stainless steel surface test. This fact shows that the effect of the substrate of the metallic surface on the CHF has no been found.

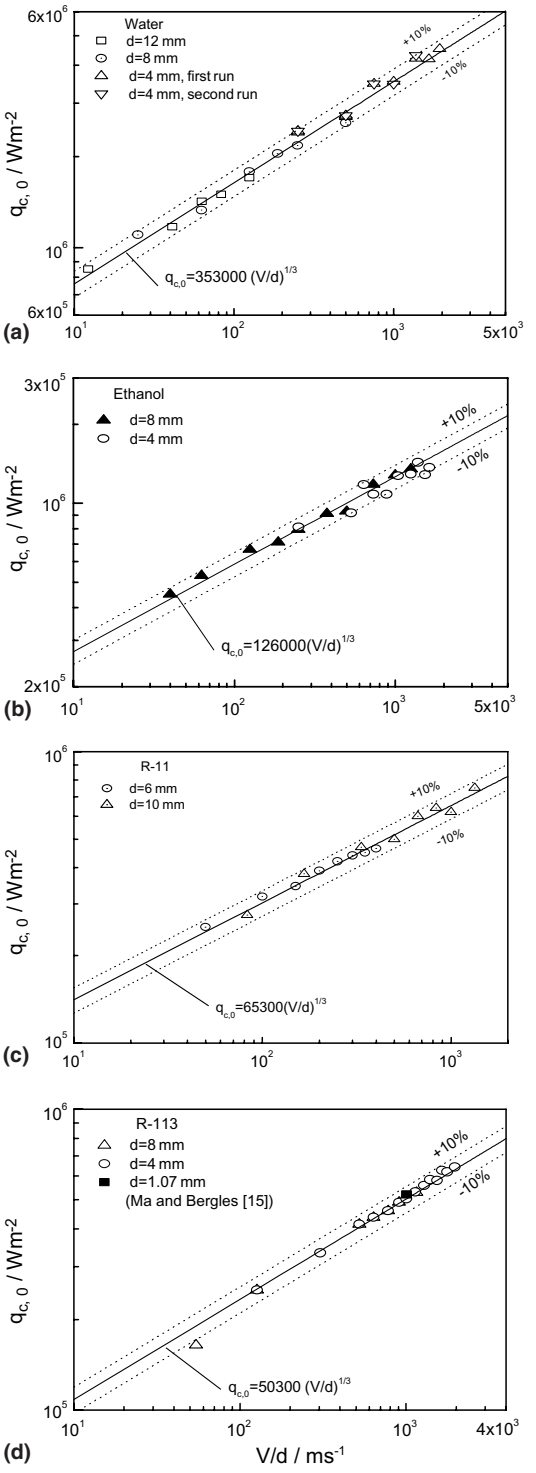

Fig. 6. Relation between the CHF and (V/d) for different saturated liquids: (a) water, (b) ethanol, (c) R-11 and (d) R-113.

Fig. 8 shows the compared results between the CHF data and the calculated values from Eq. (7). The vast

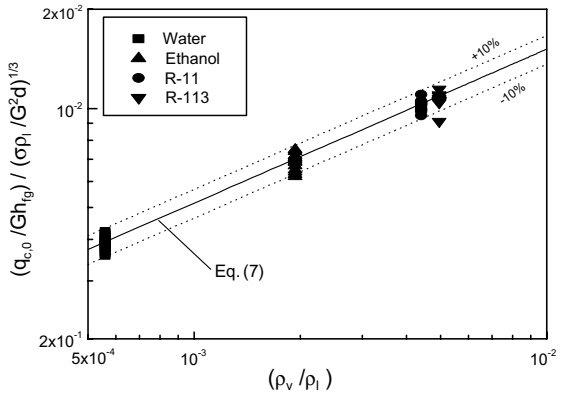

Fig. 7. Relation between the dimensionless CHF and ρ_v/ρ_l.

Table 2
Errors of the CHF predictions

Test fluid	N	$E1$	$E2$	$E3$
Water	25	−0.025	−0.039	0.002
Ethanol	20	0.005	0.021	0.001
R-11	16	0.013	0.036	0.001
R-113	21	0.019	0.022	0.001
Total	82	0.008	0.032	0.002

N: data numbers.
Average error: $E1 = \Sigma(1 - q_{cal}/q_{exp})/N$.
Mean deviation: $E2 = \Sigma|1 - q_{cal}/q_{exp}|/N$.
Standard deviation: $E3 = \Sigma(1 - q_{cal}/q_{exp})^2/N$.

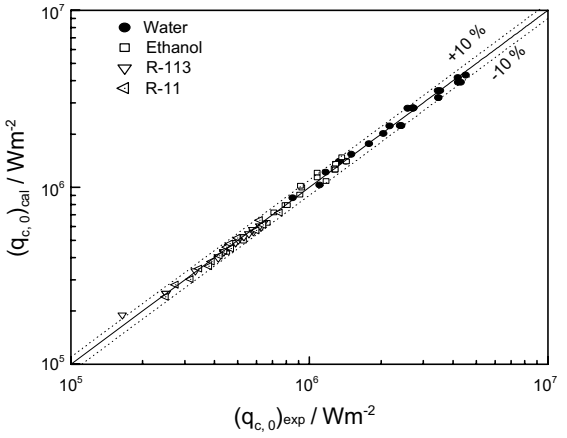

Fig. 8. Comparison between the CHF data and the calculated values from Eq. (7).

magnify of the data agree well with the predictions of Eq. (7) within the relative errors of ±10%. Eq. (7) could be recommended for predicting the CHF of jet boiling at the stagnation zone for the saturated liquids in a wide range.

4. Conclusions

An experimental investigation was carried out for predicting CHF of convective boiling for a round saturated liquids jet impinging on the horizontal jet stagnation zone. In the present study range (the impact velocities range from 0.5 m/s to 10 m/s and the diameter of the jet nozzle ranges from 3 mm to 12 mm), the following conclusions were obtained.

1. Both the impact velocity and the nozzle diameter have strong effect on CHF. Higher CHF was achieved with higher impact velocities or less nozzle diameters. The relation of $q_{c,0} \propto (V/d)^{1/3}$ is available for the saturated liquids jet.
2. There exists a good relation between the CHF data and $(\rho_v/\rho_l)^{1.4/3}$ in the present study range.
3. Dimensionless Eq. (7) correlates the CHF data and could be recommended for predicting CHF of jet boiling at the stagnation zone for various saturated liquids.

Acknowledgements

This work was supported by the national natural science foundation of China under Grant No. 50176029.

References

[1] Y. Katto, M. Shinizu, Upper limit of CHF in the saturated forced convection boiling on a heated disk with a small impinging jet, ASME J. Heat Transfer 101 (1979) 265–269.
[2] M. Monde, Burnout heat flux in saturated forced convection boiling with an impinging jet, Heat Transfer Jpn. Res. 9 (1) (1980) 31–41.
[3] M. Monde, Y. Okuma, Critical heat flux of saturated forced convection boiling on a heated disk with an impinging jet-CHF in L-regime, Int. J. Heat Mass Transfer 28 (1985) 547–552.
[4] M. Monde, Critical heat flux of saturated forced convection boiling on a heated disk with an impinging jet, ASME J. Heat Transfer 109 (1987) 991–996.
[5] Y. Katto, Critical heat flux, Adv. Heat Transfer 17 (1985) 1–65.
[6] A. Sharan, J.H. Lienhard, On predicting boiling burnout in the jet-disk configuration, ASME J. Heat Transfer 107 (1985) 398–401.
[7] Y. Katto, S. Yokoya, Critical heat flux on a disk heater cooling by a circular jet of saturated liquid impinging at the center, Int. J. Heat Mass Transfer 31 (1988) 219–227.
[8] M. Monde, T. Inoue, Critical heat flux in saturated forced convection boiling on a heated disk with multiple impinging jets, ASME J. Heat Transfer 113 (1991) 722–727.
[9] M. Monde, Critical heat flux in saturated forced convection boiling on a heated disk with one or multiple

impinging jets, Trends Heat Mass Momentum Transfer 1 (1991) 33–44.
[10] M. Monde, K. Kitajima, T. Inoue, Y. Mitsutaka, Critical heat flux in a convection subcooled boiling with an impinging jet, Heat Transfer 7 (1994) 512–518.
[11] M. Monde, Y. Mitsutake, Critical heat flux in a convection subcooled boiling with multiple impinging jets, ASME J. Heat Transfer 117 (1996) 241–243.
[12] Y. Haramura, Y. Katto, A new hydrodynamic model of critical heat flux, applicable widely to both pool and forced convection boiling on submerged bodies in saturated liquids, Int. J. Heat Mass Transfer 26 (1983) 389–399.
[13] S.K. Ishigani, J.K. Nakanishi, T.A. Hikoshichi, Boiling heat transfer for a plane water jet impinging on a hot surface, in: Proceedings of the 6th International Heat Transfer Conference, Toronto, Canada, 1978, pp. 4450–450.
[14] J.K. Nakanishi, S.K. Ishigani, T. Ochi, I. Morita, Two-dimensional water jet impinging for cooling of high temperature plate, JSME Trans. (B 46 (404) (1980) 714–724.
[15] C.F. Ma, A.E. Bergles, Jet impinging nucleate boiling, Int. J. Heat Mass Transfer 29 (1986) 1095–1101.
[16] S. Kumagai, T. Sano, T. Kamata, S. Suzuki, R. Kubo, Boiling heat transfer to an impinging jet in cooling a hot metal slab, Bull. JASM Ser. (B 60 (570) (1994) 259–263.
[17] Z.H. Liu, J. Wang, Study on film boiling heat transfer for water jet impinging on a high temperature flat plate, Int. J. Heat Mass Transfer 44 (13) (2001) 2475–2481.
[18] Z.H. Liu, Prediction of minimum heat flux for water jet boiling on a hot plate, J. Thermophys. Heat Transfer 17 (2) (2003) 159–165.
[19] Z.H. Liu, Q.Z. Zhu, Prediction of critical heat flux for convective boiling of saturated water jet impinging on the stagnation zone, Trans. ASME J. Heat Transfer 124 (6) (2002) 1125–1130.
[20] Z.H. Liu, T.F. Tong, Y.H. Qiu, Critical heat flux of steady boiling for subcooled water jet impingement on the flat stagnation zone, ASME J. Heat Transfer 126 (2) (2004) 179–183.
[21] S.S. Kutateladze, US AEC Rep., AEC-tr-3770, 1952.